Stable Lightwave Synthesized Frequency Sweeper Using Fabry–Perot Cavity Composed of Faraday Rotator Mirrors

Hiroki Takesue, Fumihiko Yamamoto, and Tsuneo Horiguchi, *Senior Member, IEEE, Member, OSA*

***Abstract*—We describe a stable lightwave synthesized frequency sweeper (LSFS) using a Fabry–Perot (FP) cavity composed of two Faraday rotator mirrors (FRM's). In the former half of this paper, we numerically simulate the behavior of amplified spontaneous emission (ASE) noise accumulations, and show that angular deviations of the FRM's can cause instability in the frequency sweep span. We also show that the span is stabilized by placing a polarizer in one of the FRM's because the FP cavity then works as a single-polarization cavity with a small transmittance fluctuation. Experimental results confirming the stability of this LSFS are provided in the latter half of this paper.**

***Index Terms*—Acoustooptic switches, birefringence, Faraday effect, optical fiber amplifiers, optical fiber communication, polarization, wavelength-division multiplexing.**

I. Introduction

ABSOLUTE lightwave frequency synthesis is a very important consideration in the field of optical measurement and many techniques for this purpose have been closely studied. The importance of these techniques is increasing recently because they can be used as lightwave frequency reference sources for optical path identification in wavelength-division multiplexing (WDM) networks [1]. Optical frequency comb generators (OFC) have been studied as one such technique [2]–[4]. This technique generates modulation sidebands which are used as frequency references. However, it is difficult to distribute these references to optical fiber networks because the broad OFC output spectrum can cause reference frequency fluctuation due to fiber nonlinearities and this limits the input power of the reference lightwave [5].

A lightwave synthesized frequency sweeper (LSFS) is another promising candidate for this application [6]–[8]. This technique has so far employed a ring cavity containing an optical coupler, an erbium-doped fiber amplifier (EDFA), a fiber-optic delay line (DL), an optical bandpass filter (BPF), and an acoustooptic frequency shifter (AOS). The continuous lightwave from a master laser, whose absolute frequency is locked to an external frequency standard, is modulated into optical pulses and launched into the fiber-optic ring through the coupler. The EDFA compensates for the optical loss in the ring so that the pulse can circulate around the ring many times. The pulse undergoes a frequency shift with the AOS in each circulation. As a result, we can obtain an optical pulse train whose frequency is swept stepwise. The frequencies of the pulses are precisely determined by that of the master laser and the frequency shift of the AOS. The fluctuation of the AOS frequency shift is very small compared with that of a lightwave frequency, so these pulses can be used as lightwave frequency references. When we distribute these pulses to optical fiber networks, the frequency fluctuation due to fiber nonlinearities hardly occurs because each pulse has a single frequency and its time width is relatively large ($\sim\mu$s). Therefore, we can use these pulses for time shared lightwave reference frequency distribution in WDM networks [8].

In the LSFS, the frequency sweep span is proportional to the number of signal pulse circulations in the ring cavity, which is limited by the accumulation of amplified spontaneous emission (ASE) noise from the EDFA. There has already been a problem regarding the stability of the frequency sweep span. When the birefringence of a ring cavity with a polarization dependent loss (PDL) changes, the cross-gain saturation effect occurs between the circulating signal pulse and the ASE noise component which is polarized orthogonally to the signal, and it causes a change in the span [7]. Construction of the ring with polarization maintaining (PM) components seems to eliminate this polarization fluctuation induced instability. However, the use of costly PM fiber makes the whole system expensive. In addition, it is difficult to fabricate PM components and the state of polarization (SOP) of circulating lightwave sometimes changes at such components.

We have already reported another effective method for stabilization: an LSFS containing a fiber Lyot depolarizer with a large birefringence [9]. The large birefringence of the depolarizer together with the frequency change of the circulating pulse causes constant changes in the SOP of the pulse, which prevents the cross gain saturation effect from arising. Although this method is more practical than to use a PM ring, this also has a drawback: the SOP's of output pulses are scrambled by the depolarizer. Therefore, a sophisticated technique such as polarization diversity is needed when we use this LSFS, for example, with a heterodyne detection system.

As an alternative stabilization method, a Fabry–Perot (FP) cavity composed of two Faraday rotator mirrors (FRM's) has been applied to the LSFS [10], [11]. The stabilization with this method is based on the cancellation of PDL in the cavity, by which the cross gain saturation effect between the two polarization eigenmodes is suppressed. The effectiveness of PDL cancellation in the cavity was confirmed experimentally when the

Manuscript received May 15, 1999; revised October 18, 1999.

The authors are with NTT Access Network Service Systems Laboratories, Ibaraki-ken 305-0805, Japan.

Publisher Item Identifier S 0733-8724(00)02196-4.

cavity was used as a fiber laser [12] and an all-optical gain-clamped amplifier [13]. However, the suppression mechanism as an LSFS has not been investigated in detail.

An FP cavity composed of FRM's has already been theoretically analyzed as a fiber laser by Takushima et al. [14]. They assumed that the cavity components had no PDL's except for the polarizer inserted in the cavity and calculated the cavity transmittance for the two polarization modes. However, when an FP cavity is used as an LSFS, it is essential to take the cavity PDL into consideration when explaining the decrease in the number of pulse circulations caused by the cross gain saturation effect between the polarization modes. We will explain this in detail in Section II. Therefore, we require a different analysis of the FP cavity.

In this paper, we describe an LSFS using an FP cavity composed of FRM's. This LSFS features a very stable frequency sweep span and the SOP of the output pulses is consistent. In Section II, we analyze this FP cavity as an LSFS and estimate the stability of the frequency sweep span. Here we also show that the span stability is further improved by inserting a polarizer between the Faraday rotator and the mirror in one of FRM's. In Section III, we provide experimental results which directly confirm the high span stability. In Section IV, we describe a method for enlarging the frequency sweep span and an LSFS system application. In Section V, we summarize this paper.

II. Theory: Behavior of Pulse Circulation in FP Cavity Composed of FRM's

When an optical cavity contains a component with a PDL, it has two polarization eigenmodes with different optical losses. Hereafter, we define "PDL" as including the polarization dependent gain (PDG) of a gain medium in the cavity. If the gain medium is operated as an optical amplifier in the saturation mode, the two modes in the cavity are coupled through the amplifier gain. In this situation, the cross gain saturation effect occurs between these modes. This effect can seriously affect the signal pulse circulation. First we explain this effect using simple equations.

We assume that the lightwave circulating in the cavity has two polarization modes x and y. These two modes are not exactly orthogonal because the cavity that we are considering has a PDL. However, the PDL remaining in our cavity is very small as we will explain in this section, so the two modes can be approximated as being orthogonal. The validity of this approximation is discussed in Appendix A. In an optical cavity containing an optical amplifier operated in the saturation mode, it is valid to assume that the power is constant for each circulation when calculating the number of pulse circulations [15]. Therefore, the following relationship exists among P_x: the optical power of mode x, P_y: that of mode y, and P_c: total optical power

$$P_x^i + P_y^i = P_c \tag{1}$$

Here i denotes the circulation number. We assume that the cavity has a PDL: i.e. $L_x \neq L_y$ (L_j: the round-trip transmittance of the cavity for mode j ($=x, y$)). The EDFA gain G is related to the above powers by using L_x and L_y as follows:

$$G^i \left(L_x P_x^i + L_y P_y^i\right) = P_c. \tag{2}$$

By using (1) and (2), the net gain of the cavity for mode x can be expressed as

$$L_x G^i = \frac{1}{1 + \frac{L_y - L_x}{L_x} \frac{P_y^i}{P_c}}. \tag{3}$$

The above equation is valid for mode y if we exchange subscripts x and y. If we assume $L_x > L_y$, (3) shows that the net gain for mode x exceeds 1. At the same time, the net gain for mode y falls below one. Equation (3) also shows that the net gain for mode x becomes larger as P_y^i becomes smaller. Therefore, if L_x is larger than L_y, P_x^i grows increasingly quickly as the pulse circulates. When the SOP of the signal pulse is in mode x, it can circulate in the cavity many times. However, a change in the cavity birefringence can change the signal SOP into mode y. Then the ASE noise component in mode x grows and the number of pulse circulations greatly decreases. Thus, the PDL of the cavity causes the cross gain saturation effect between the polarization modes, which in turn causes the instability of the number of pulse circulations.

Ideally, an FP cavity composed of FRM's with rotation angles of $\pi/4$ has no residual PDL even when the cavity contains components with PDL's, as we will explain later. Therefore, the use of such a cavity seems to realize stable pulse circulations. However, the FRM rotation angles generally deviate from $\pi/4$, so the FP cavity has a residual PDL, which may induce instability.

Based on this idea, we analyze the stability of the signal pulse circulation in an FP cavity composed of FRM's in this section. We first calculate the residual PDL using Jones matrixes. We then provide the results of a numerical calculation which shows that the residual PDL can cause the cross gain saturation effect between the polarization modes and cause a considerable deterioration in the number of pulse circulations. Finally we describe an effective way to stabilize the number by inserting a polarizer between the Faraday rotator and the mirror in one of the FRM's.

A. Residual PDL in FP Cavity Composed of FRM's

Fig. 1 shows our model for analyzing an FP cavity composed of two FRM's. In this model, the x- and y-axes are fixed even when the direction of the lightwave propagation is reversed. The matrix for the Faraday rotator with a polarization rotation angle of Θ is expressed as

$$F(\Theta) = \begin{pmatrix} \cos\Theta & \sin\Theta \\ -\sin\Theta & \cos\Theta \end{pmatrix}. \tag{4}$$

Matrix B, which expresses the linear birefringence for the left direction in the cavity, is generally expressed as $\begin{pmatrix} a & b \\ -b^* & a^* \end{pmatrix}$ using two complex numbers a and b. Here, we do not include the effect of the cavity loss in B, so the relationship $|a|^2 + |b|^2 =$

1 is satisfied. Therefore, B can be changed into the following expression using three real variables $\theta, \Delta\phi_1$ and $\Delta\phi_2$.

$$B(\theta,\Delta\phi_1,\Delta\phi_2)=\begin{pmatrix} e^{-i\frac{\Delta\phi_1}{2}} & 0 \\ 0 & e^{i\frac{\Delta\phi_1}{2}} \end{pmatrix}\begin{pmatrix} \cos\theta & \sin\theta \\ -\sin\theta & \cos\theta \end{pmatrix} \times \begin{pmatrix} e^{-i\frac{\Delta\phi_2}{2}} & 0 \\ 0 & e^{i\frac{\Delta\phi_2}{2}} \end{pmatrix}. \quad (5)$$

The birefringence matrix for the right direction is expressed by the transpose matrix ${}^tB$. We can realize an arbitrary cavity birefringence by changing the variables $\theta, \Delta\phi_1$ and $\Delta\phi_2$. We assume that the sum of the component PDL's is α dB. The matrix for the single-pass PDL in the cavity is expressed using the following matrix P:

$$P=\begin{pmatrix} 1 & 0 \\ 0 & 10^{-\frac{\alpha}{20}} \end{pmatrix}. \quad (6)$$

We set the input and output ports as in Fig. 1. Then the matrix for a round-trip of the cavity can be expressed as

$$U(\Theta_1,\Theta_2,\theta,\Delta\phi_1,\Delta\phi_2,\alpha) = {}^tBP(\alpha)F(\Theta_1)^2P(\alpha)BF(\Theta_2)^2 \quad (7)$$

where Θ_1 and Θ_2 are the rotation angles of the Faraday rotators on the left and right sides, respectively. The second powers of the absolute values of the eigenvalues for matrix U are proportional to the cavity transmittance for the polarization eigenmodes, while the arguments of the eigenvalues denote the phase change of the eigenmodes for one round-trip in the cavity.

When the cavity is operated as a fiber laser, the difference between the two arguments causes a serious effect, namely mode hopping between the two eigenmodes [14]. However, when the cavity is used as an LSFS, the above difference has no effect on the pulse circulation because the circulating signal pulse does not oscillate in the cavity. Therefore, we only need to consider the second powers of the eigenvalues. Here we introduce the residual PDL of the cavity α_r, which corresponds to the PDL for a round-trip of the cavity, expressed as:

$$\alpha_r = |20\log(\lambda_1/\lambda_2)| \quad (8)$$

where λ_1 and λ_2 are the absolute values of the eigenvalues of U.

When ideal Faraday rotators are used ($\Theta_1 = \Theta_2 = \pi/4$), matrix U is reduced to

$$U=\begin{pmatrix} 10^{-\frac{\alpha}{20}} & 0 \\ 0 & 10^{-\frac{\alpha}{20}} \end{pmatrix}. \quad (9)$$

In this case, the eigenvalues degenerate, which means the residual PDL α_r becomes 0 dB. Thus, no cross gain saturation effect occurs between the polarization modes and the number of pulse circulations is stabilized even when the cavity birefringence fluctuates. In addition, if the change in the cavity birefringence takes much longer than the round-trip time of the cavity, the effect of the birefringence is canceled and the SOP's of the output pulse train become consistent.

However, since Faraday rotators use the magnetooptic effect, the rotation angles of Faraday rotators can be perturbed by a change in the magnetic field strength and generally deviate slightly from $\pi/4$. Therefore, the PDL effect does not disappear in such a cavity and a change in the number of pulse circulations is induced by the fluctuation of the cavity birefringence. Furthermore, the consistency of the SOP's of an output pulse train will also be lost.

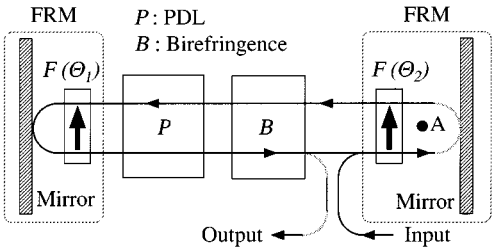

Fig. 1. Model for calculating residual PDL.

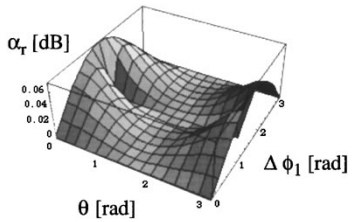

Fig. 2. Residual PDL at various states of cavity birefringence. A component PDL sum of 0.5 dB and angular deviations of 2° for both FRM's are assumed.

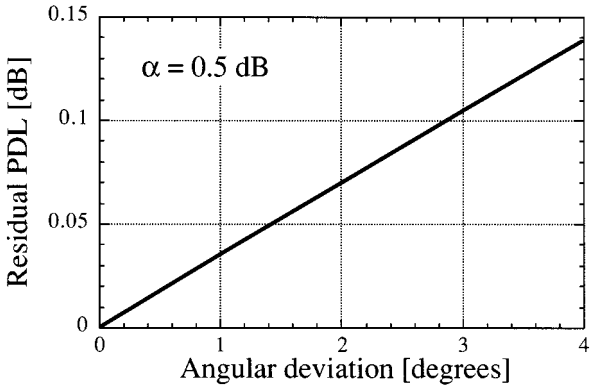

Fig. 3. Residual PDL for worst cavity birefringence as a function of the angular deviation of the Faraday rotators. The sum of the component PDL's is 0.5 dB.

In the following, we estimate the residual PDL α_r in the FP cavity assuming that the angular deviations from $\pi/4$ of both FRM's are δ (i.e. $\Theta_1 = \Theta_2 = \pi/4 - \delta$). In our experimental setup, δ and the sum of the component PDL's α are estimated to be 2° and 0.5 dB, respectively. First we changed $\Delta\phi_1$ and θ of the birefringence matrix B assuming $\Delta\phi_1 = \Delta\phi_2$ and calculated α_r using (7) and (8); Fig. 2 shows the result. This figure clearly shows that the residual PDL depends on the birefringence.

Fig. 3 shows the residual PDL with respect to the angular deviations of the Faraday rotators. Here, we assumed α to be 0.5 dB and set the birefringence matrix so that the residual PDL became maximum. The figure shows that the residual PDL increases almost linearly with the angular deviations of the Faraday rotators. This figure also implies that the maximum value of α_r is approximately 0.07 dB in our experimental setup

with angular deviations of 2°. In the next subsection, this result will be used to estimate the impact of the residual PDL on the number of pulse circulations.

B. Cross-Gain Saturation Effect in FP Cavity with Residual PDL

In this subsection, we numerically calculate the number of signal pulse circulations using the residual PDL estimated in the previous section.

In Appendix B, we show our simulation procedure. By solving (14), (17), and (18) numerically, we can calculate the power of the signal pulse and the ASE noise which are circulating in the FP cavity. Table I shows the parameter values we used in the numerical simulations, which are based on values measured in our experimental setup. The two polarization eigenmodes of the FP cavity are denoted by subscript x and y. The transmittance for mode x is larger than that of mode y.

The best and worst signal pulse SOP can be realized by setting $P^0_{sx} = P_c$ and $P^0_{sy} = P_c$, respectively. Here P_c denotes the total optical power and P^0_{sj} is the input pulse power in polarization mode j $(j = x, y)$. In this numerical simulation, we define the number of pulse circulations as the number at which the ASE noise level reaches 98% of the total power level.

We show the numerical results of the ASE noise output power as a function of the signal pulse circulation number in Fig. 4. The residual PDL was set at 0.07 dB, which is the worst-case residual PDL for our experimental setup calculated in the previous subsection. When the pulse SOP is in mode x (best SOP), the pulse can circulate 346 times. However, the number decreases to 295 when the signal SOP is in mode y (worst SOP). This change corresponds to a change in the frequency sweep span of approximately 15%. In addition, the ratio of signal pulse power to ASE noise power deteriorates for the whole pulse train. Thus, it is obvious that a very small residual PDL of 0.07 dB can considerably affect the number of pulse circulations.

We then calculated the number of pulse circulations at the worst SOP as a function of the residual PDL. The result is shown in Fig. 5. From this result, for example, if we want to suppress the fluctuation in the frequency sweep span to 5% (corresponding to 329 pulse circulations at the worst SOP), the residual PDL should be less than approximately 0.03 dB. From Fig. 3, we have to suppress the angular deviations to less than approximately 0.8° to achieve that small residual PDL. This is difficult to realize in practice.

Thus, even when using an FP cavity composed of the FRM's, we need to meet very severe demands for small angular deviations as regards the FRM's and a small component PDL to avoid the instability caused by the cross gain saturation effect between polarization eigenmodes.

C. Stabilization in Number of Pulse Circulations by Inserting Polarizer

An effective way to avoid the cross gain saturation effect between polarization modes is to insert a polarizer between the Faraday rotator and the mirror of one of the FRM's (for example, point A in Fig. 1). This polarizer removes the polarization component which is orthogonal to its axis and the SOP of the circulating lightwave is fixed in one state. Consequently, there is no cross gain saturation effect between the two polarization modes in this cavity. By setting the input pulse SOP so that it passes through the polarizer at the first circulation, we can realize stable pulse circulations with no cross gain saturation effect.

In this case, the SOP of the pulse changes slightly after one round-trip in the FP cavity because of the angular deviations of the FRM's. This leads to an excess loss at the polarizer. The amount of SOP change depends on the cavity birefringence, so the cavity transmittance for the circulating lightwave changes if the cavity birefringence fluctuates. Therefore, we calculated the change in the cavity transmittance and estimated how the change affects the number of pulse circulations.

TABLE I
PARAMETER VALUES FOR NUMERICAL SIMULATIONS

n_{sp}: spontaneous emission noise factor	1.5
B: 3 dB bandwidth of BPF	5 nm
P_c: total optical power	0.1 mW
Δf: AOS frequency shift	120 MHz
Input pulse wavelength	1550 nm
L(f_c): single-pass transmittance of cavity at center frequency f_c	0.1
Initial frequency deviation from BPF center frequency	20 GHz

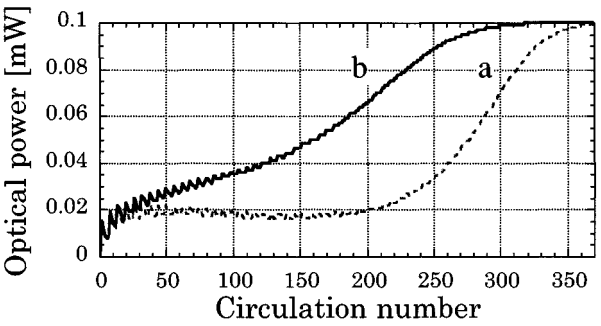

Fig. 4. ASE noise power as a function of signal pulse circulation number when the FP cavity is composed of FRM's without a polarizer. (a) Best signal SOP and (b) worst signal SOP. Residual PDL = 0.07 dB.

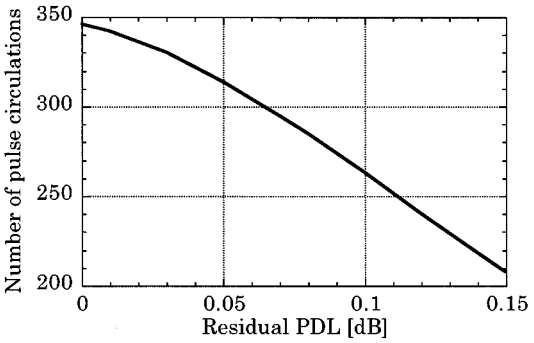

Fig. 5. Numerical result of the number of pulse circulations for the worst SOP of the circulating lightwave as a function of residual PDL.

When we placed a polarizer at point A in Fig. 1, the matrix for one round-trip of the FP cavity U' is expressed as

$$U'(\Theta_1, \Theta_2, \theta, \Delta\phi_1, \Delta\phi_2, \alpha) = {}^tBP(\alpha)F(\Theta_1)^2P(\alpha)BF(\Theta_2)D^2F(\Theta_2), \quad (10)$$

where D is the matrix for the polarizer and expressed as follows:

$$D = \begin{pmatrix} 1 & 0 \\ 0 & 0 \end{pmatrix} \quad (11)$$

U' has two eigenvalues, one of which is zero, and the second power of the other corresponds to the cavity transmittance for the circulating lightwave. We changed θ, $\Delta\phi_1$ and $\Delta\phi_2$, and calculated the minimum and maximum values of the cavity transmittance. Here, $\delta = 2^\circ$ and $\alpha = 0.5$ dB are assumed as in the previous simulation. As a result, the difference between the minimum and maximum values of the cavity transmittance was calculated to be approximately 0.10 dB.

Using this figure, we numerically calculated the ASE noise power circulating in the FP cavity when the cavity transmittance reached minimum and maximum. By multiplying 0 by L_x in (14), (17), and (18) which are shown in Appendix B, we can include the effect of the polarizer which transmits y polarization. The maximum and minimum values of the cavity transmittance can be realized by setting α_r at 0 and 0.10, respectively.

We show the result for the minimum transmittance in Fig. 6 (curve a). The number of pulse circulations is 351, which is almost the same as that for the maximum transmittance. This means the small fluctuation in the cavity transmittance of 0.10 dB hardly affects the number of pulse circulations. Curve a is also similar to the curve for the best polarization signal pulse in the FP cavity without a polarizer with 346 pulse circulations. Thus, the number of pulse circulations is kept high and its fluctuation is suppressed using the FP cavity with a polarizer. To show the improvement in the stability of the number of pulse circulations, the result for the worst polarization signal pulse in the FP cavity without a polarizer is also shown in Fig. 6 (curve b).

In addition to providing pulse circulation stability, this configuration has another merit: the SOP's of the output pulses can be fixed by the polarizer. This feature will make the LSFS easy to use for applications which require polarization consistency.

Thus, an FP cavity composed of FRM's with a polarizer can work as a single-polarization cavity with a small transmittance fluctuation. With this cavity, we can realize a practical LSFS with stable pulse circulations and a single-polarization output.

III. Experiments

In this section, we describe experiments which proved the good performance of the LSFS with an FP cavity composed of FRM's. We report experimental results that confirmed its high stability and which are in accordance with the simulated results in Section II.

Fig. 7(a) shows the configuration of the LSFS with the FP cavity configuration. The cavity is composed of a 9:1 coupler, two FRM's, a dispersion shifted fiber (DSF) used as a DL, a BPF with a 3 dB bandwidth of 5 nm, a bidirectional EDFA, and an AOS with a -120 MHz frequency shift. The round-trip

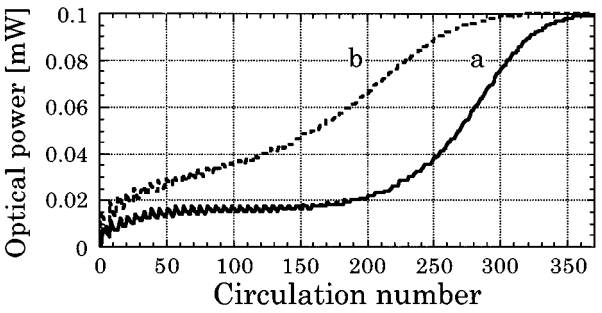

Fig. 6. ASE noise power as a function of signal pulse circulation number when using FP cavities composed of FRM's with and without a polarizer. (a) FP cavity with polarizer, (b) FP cavity without polarizer (worst SOP).

time and loss of the cavity are approximately 6.5 μs and 21 dB, respectively. We used two types of FRM for FRM1: FRM1a and FRM1b. FRM1a and FRM2 consist of a Faraday rotator and a mirror, and are coupled with DSF's. FRM1b consists of a Faraday rotator module, a PM fiber-polarizer and a mirror. The components of FRM1b are connected through PANDA fibers. For the Faraday rotators used in these FRM's, we estimated the deviations of the one-pass Faraday rotation angles from 45° to be approximately 2.0° in the 1.55-μm wavelength band. The sum of the component PDL's is approximately 0.5 dB. This is mainly due to the PDL's of the AOS and the BPF, but also includes the PDG of the gain medium, which is approximately 0.1 dB. In the following experiments using FRM1b, we set the SOP of the input signal pulse to maximize the power transmitted from the polarizer.

The wavelength of the master laser was stabilized at 1550.2 nm using a $^{13}C_2H_2$ absorption line as an absolute frequency reference. The continuous lightwave from the master laser was modulated into an optical pulse and input into the cavity through the input port of the coupler. The pulse was reflected and its SOP rotated by 90° with FRM1 before passing through the coupler and the DL. The pulse then underwent spectral filtering with the BPF to reduce the ASE noise, was amplified with the EDFA, was frequency shifted by -120 MHz with the AOS, and finally reached FRM2. The pulse was reflected by FRM2 with the SOP rotated by 90° and retraced its path. When the pulse reached the coupler again, part of the pulse power was output. As a result, we obtained an optical pulse train whose frequency was swept in -240 MHz steps.

Fig. 8 shows the typical output pulse train when we used the FP cavity with FRM1b. The upper trace corresponds to the signal pulse power. The width of the input pulse was set a little shorter than the round-trip time of the FP cavity, and so we were able to monitor the ASE noise level between successive output signal pulses (the lower trace). The maximum number of pulse circulations was approximately 350 ($250\ \mu s \times 9.2$ div./$6.5\ \mu s$), which corresponds to a frequency sweep span of 84 GHz. The fluctuations seen in the signal pulse power levels are assumed to be interference noise caused by reflections from the connectors or surfaces of the components in the cavity. Therefore, this noise may be reduced by splicing those connecting points.

We estimated the stability of the frequency sweep span when the birefringence was changed. We inserted a PC in a cavity and rotated the quarter-wave plate (QWP) of the PC, by which

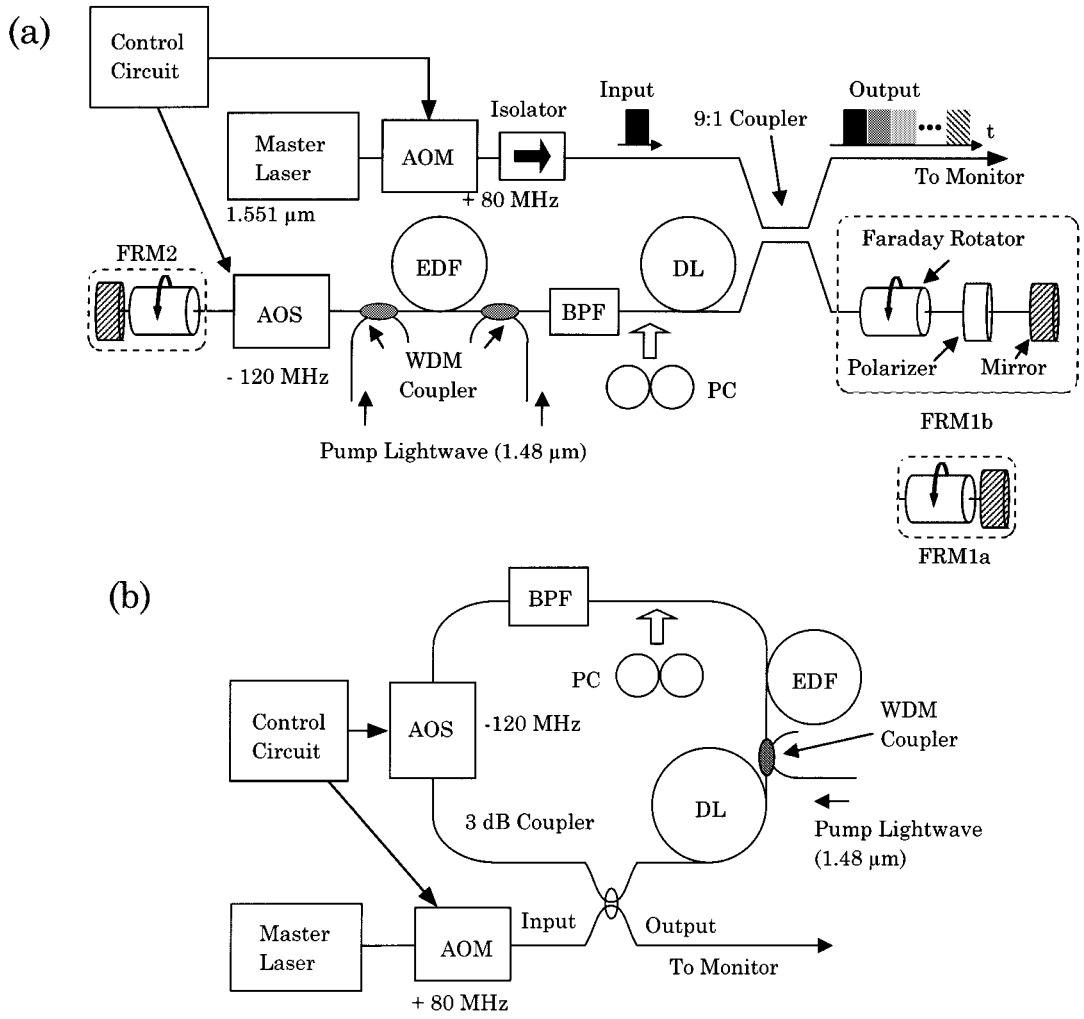

Fig. 7. Experimental setup: (a) FP cavity composed of FRM's and (b) ring cavity.

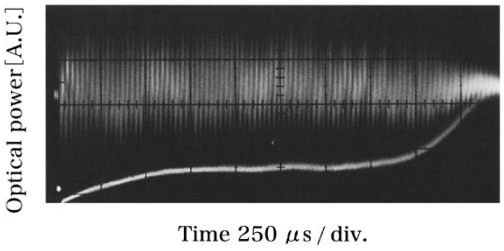

Fig. 8. Typical output pulse train when an FP cavity composed of FRM's with a polarizer was used. Upper trace: Total optical power. Lower trace: ASE noise power.

we changed the cavity birefringence. Then we plotted the frequency sweep span with respect to the rotation angle. For comparison, the same experiment was undertaken for three kinds of optical cavities: the FP cavity with FRM1a, the FP cavity with FRM1b, and the ring cavity shown in Fig. 7(b). The ring cavity contained the same AOS and BPF as the FP cavities. The maximum values of the frequency sweep spans for each cavity had slight variations. The optical losses of these cavities were different and this resulted in such variations. The maximum spans for each cavity were 92 GHz for the ring cavity, 84 GHz for the FP cavity without a polarizer (using FRM1a), and 90 GHz for the FP cavity with a polarizer (FRM1b). Therefore, we normalized their frequency sweep spans by their maximum values. The results are shown in Fig. 9. With the ring, the change in the span was more than 60%. By using the FP cavity with FRM1a, the fluctuation in the span became smaller. However, the span still changed by more than 30%. By contrast, when we used the FP cavity with FRM1b, the fluctuation was considerably suppressed to 9%. This result confirms the good stability of the sweeper using an FP cavity composed of FRM's with a polarizer. The fluctuations in the spans for the two FP cavities were larger than the values calculated in Section II. However, these results are generally in good agreement with the numerical results. The discrepancy between the numerical and experimental values of the spans may be due to errors that occurred when counting the numbers of pulse circulations. These errors were probably caused by interference noise on the output signal pulses.

We then confirmed the long-term stability of the pulse circulation. We used the FP cavity with FRM1b and monitored a pulse which underwent a 60.24 GHz frequency shift (corresponding to 251 circulations) for 12 hours in 0.5-hour steps and plotted the ratio of the signal pulse power to the ASE noise power. Fig. 10 shows the results. The ratio of the signal pulse

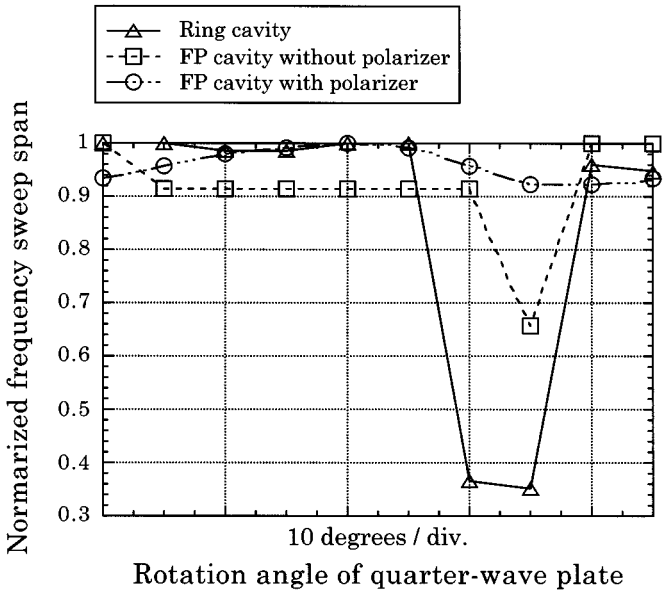

Fig. 9. Frequency sweep spans at various QWP settings for the ring cavity, the FP cavity without a polarizer and the FP cavity with a polarizer.

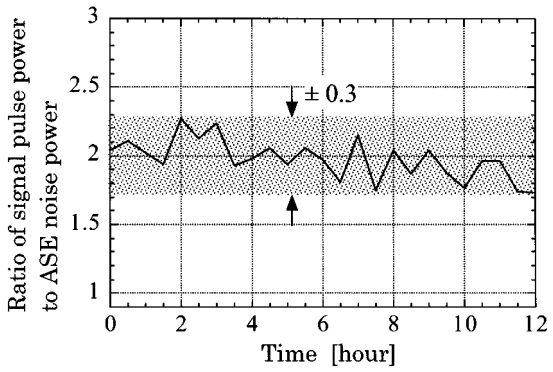

Fig. 10. Temporal change in ratio of signal pulse power to ASE noise power at 251st pulse.

power to the ASE noise power was 2.0 on average, and its change was within ± 0.3. Therefore, we can use this pulse as a stable lightwave frequency reference for a long period.

Finally, we confirmed the consistency of the SOP of the output pulse train. We monitored the pulse train after it had passed through a polarization controller (PC) and a polarizer. The monitored waveform of the pulse train almost disappeared when we adjusted the PC, and could be regenerated by rotating the polarizer through 90°. This means the SOP's of the pulses were fixed in one state.

IV. Discussion

The frequency sweep span of our LSFS is currently about 100 GHz. However, this span is not large enough for WDM network applications. Therefore, we need to increase the number of pulse circulations to further enlarge the span. One effective way to achieve this is to use a synchronously-tuned BPF in an LSFS. We have already employed this method in a ring cavity and achieved a 1.1-THz span [16]. However, an instability which is due to the cross gain saturation effect between polarization modes was also observed in this LSFS. By applying a synchronously-tuned BPF to the FP cavity composed of FRM's, we can expect a stable LSFS with a frequency sweep span of more than 1 THz.

An interesting application of this sweeper is as a continuous-wave (CW) frequency synthesizer based on discrete-time negative frequency feedback [17]. In addition to the stability of its frequency sweep span, an LSFS using an FP cavity composed of FRM's has another merit, namely the consistency of the SOP's of its output pulse train. Thanks to this characteristic, we do not need to use sophisticated (and expensive) techniques such as polarization diversity receivers at the heterodyne detection part of the CW frequency synthesizer.

V. Conclusion

We discussed a stable LSFS using an FP cavity composed of FRM's. We calculated the residual PDL in the cavity containing FRM's with angular deviations and showed that it induces the cross gain saturation effect between the polarization modes, which leads to a fluctuation in the frequency sweep span. We also showed that the fluctuation is effectively suppressed by using a single-polarization FP cavity with a small transmittance fluctuation, which is realized by inserting a polarizer in one of the FRM's. We then showed experimental results which directly confirmed the stability of the LSFS. With a further enlargement of the span, we can expect that this LSFS will be used as a lightwave frequency reference source for WDM networks.

Appendix A
Validity of the Approximation of the Polarization-Mode Orthogonality

The FP cavity described by (7) has a PDL. Therefore, the polarization eigenmodes of the cavity are not exactly orthogonal. However, the residual PDL in the cavity is small (maximum 0.07 dB), so we expect the relationship between the two modes to be nearly orthogonal. In this appendix, we show that the deviation from polarization-mode orthogonality of our cavity is very small and so can be disregarded.

We assume that the eigenvectors of U are $\vec{v_1}$ and $\vec{v_2}$, which satisfy $\vec{v_1}^2 = \vec{v_2}^2 = 1$. The powers of the two modes are p_1 and p_2, respectively. The total power in the cavity is expressed as

$$\begin{aligned}|\sqrt{p_1}\vec{v_1} + \sqrt{p_2}\vec{v_2}|^2 &= (\sqrt{p_1}\vec{v_1} + \sqrt{p_2}\vec{v_2})(\sqrt{p_1}\vec{v_1} + \sqrt{p_2}\vec{v_2})^* \\ &= p_1 + p_2 + 2\sqrt{p_1 p_2}\,\mathrm{Re}(\vec{v_1}\vec{v_2}^*). \qquad (12)\end{aligned}$$

If the two eigenmodes are orthogonal, $\vec{v_1} \cdot \vec{v_2}^*$ becomes zero. The calculated $\mathrm{Re}(\vec{v_1} \cdot \vec{v_2}^*)$ for our cavity expressed by (7) is 0.029 even when we set $\theta, \Delta\phi_1$ and $\Delta\phi_2$ to maximize the value. Thus, the third term of (12) is very small compared with the total optical power. Therefore, we conclude that it is valid to approximate that the two polarization modes are orthogonal.

Appendix B
Basic Model for Numerical Simulations of Cross Gain Saturation Effect Between Two Polarization Eigenmodes

An optical pulse circulating in an optical cavity has already been studied through numerical simulations in [15]. However,

$$G^i = \frac{P_c}{\sum_j^{x,y}\left(L_j\left(f_s^i+2\Delta f\right)L_j\left(f_s^i\right)P_{sj}^i\left(f_s^i\right)+\int_{f_c-B/2}^{f_c+B/2}L_j(f+2\Delta f)\left[L_j(f)G^i p_{nj}^i(f)+n_{\rm sp}\frac{G^i-1}{G^i}h\nu\right]df\right)}. \quad (18)$$

a cavity with only one polarization mode was analyzed in that case. In this appendix, we extend this method to an FP cavity with two polarization modes. We derive propagation equations for the signal and the ASE noise circulating in the FP cavity.

Fig. 11 shows the model for the analysis. Here we assume that the total power circulating in the ring remains constant, as mentioned in Section II. We neglect the effect of polarization mode dispersion, which is almost eliminated after one round-trip in the cavity thanks to the FRM's. For the numerical simulations, we introduce the following notations.

- P_c: Total optical power.
- P_{sj}^0: Input pulse power in the polarization mode j $(j = x, y)$.
- P_{sj}^i: Signal pulse power in polarization mode j at the ith circulation number.
- $p_{nj}^i(f)$: Partial ASE noise power density around frequency f in polarization mode j at the ith circulation number.
- P_{nj}^i: Total ASE noise power in polarization mode j at the ith circulation number.
- G^i: Saturated gain of an EDFA at the ith circulation number.
- $L_j(f)$: Single-pass optical transmittance of the cavity for polarization mode j at frequency f.
- f_s^i: Frequency of the signal pulse at the ith circulation number.
- f_c: Center frequency of the BPF.
- Δf: Frequency shift of the AOS.
- B: 3 dB bandwidth of the BPF.

If we assume the BPF has Lorentzian characteristics and includes the effect of the residual PDL, $L_j(f)$ can be written as

$$L_x(f) = \frac{L(f_c)}{1+\frac{f-f_c}{B/2}}$$

$$L_y(f) = 10^{-\alpha_r/20}\times\frac{L(f_c)}{1+\frac{f-f_c}{B/2}}$$

where $L(f_c)$ is the transmittance at the center frequency of the BPF for mode x and α_r is the residual PDL of the cavity in dB units. We assume that mode x has the larger transmittance.

From the assumption of constant power approximation, we obtain,

$$P_c = \sum_j^{x,y}\left(P_{sj}^i+P_{nj}^i\right) = \sum_j^{x,y}\left(P_{sj}^{i+1}+P_{nj}^{i+1}\right). \quad (13)$$

In this simulation, we assume that the gain medium with the mirror on the left in Fig. 11 works as one reflection-type EDFA. The propagation of the signal pulse power in mode j $(j = x, y)$ is expressed using the following equation:

$$P_{sj}^{i+1}\left(f_s^i+2\Delta f\right) = L_j\left(f_s^i+2\Delta f\right)L_j\left(f_s^i\right)G^iP_{sj}^i\left(f_s^i\right). \quad (14)$$

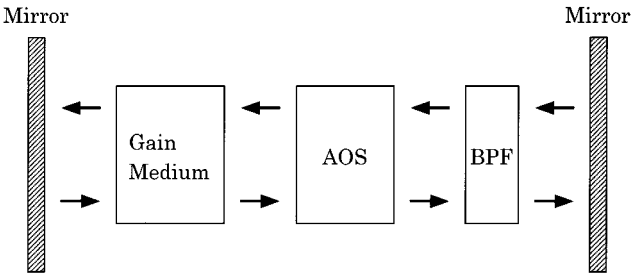

Fig. 11. Model for numerical simulation of the cross gain saturation effect between polarization modes.

Similarly, the next equation represents the propagation of the partial ASE noise power in mode j.

$$p_{nj}^{i+1}(f+2\Delta f) = L_j(f+2\Delta f)L_j(f)G^ip_{nj}^i(f)hfill + \frac{L_j(f+2\Delta f)S^i}{B}. \quad (15)$$

Here, S^i is the ASE power generated from the EDFA for each polarization mode. This is defined by [5]

$$S^i = n_{\rm sp}\left(G_k^i-1\right)h\nu B \quad (16)$$

where $n_{\rm sp}$ is a spontaneous emission noise factor and $h\nu$ is the photon energy. Using (15), the total ASE noise power in mode j is given by

$$P_{nj}^i = \int_{f_c-B/2}^{f_c+B/2}p_{nj}^i(f)\,df. \quad (17)$$

Using (13), (14), and (17), the gain for the ith circulation is calculated to be (18) shown at the top of the page.

ACKNOWLEDGMENT

The authors would like to thank Dr. K. Shimizu of NTT Basic Research Laboratories for fruitful discussions on lightwave frequency synthesis techniques and Dr. T. Sugie for his encouragement of our research.

REFERENCES

[1] K. Sato, S. Okamoto, and H. Hadama, "Network performance and integrity enhancement with optical path layer technologies," *IEEE J. Select. Areas Commun.*, vol. 12, pp. 159–170, Jan. 1994.

[2] M. Kourogi, K. Nakagawa, and M. Ohtsu, "Wide-span optical frequency comb generator for accurate optical frequency difference measurement," *IEEE J. Quantum Electron.*, vol. 29, pp. 2693–2701, Oct. 1993.

[3] L. R. Brothers, D. Lee, and N. C. Wong, "Terahertz optical frequency comb generation and phase locking of an optical parametric oscillator at 665 GHz," *Opt. Lett.*, vol. 19, no. 4, pp. 245–247, 1994.

[4] H. Yasaka, Y. Yoshikuni, K. Sato, H. Ishii, and H. Sanjoh, "Multiwavelength light source with precise frequency spacing using mode-locked semiconductor laser and arrayed waveguide grating filter," in *Proc. Opt. Fiber Commun. Conf. OFC 96*, paper FB2.
[5] G. Agrawal, *Nonlinear Fiber Optics*. New York: Academic, 1989.
[6] T. G. Hodgkinson and P. Coppin, "Pulsed operation of an optical feedback frequency synthetiser," *Electron. Lett.*, vol. 26, no. 15, pp. 1155–1157, 1990.
[7] K. Shimizu, T. Horiguchi, and Y. Koyamada, "Frequency translation of light waves by propagation around an optical ring circuit containing a frequency shifter: I. Experiment," *Appl. Opt.*, vol. 32, no. 33, pp. 6718–6726, 1993.
[8] K. Aida and K. Nakagawa, "Time shared lightwave reference frequency distribution for photonics networks," *J. Lightwave Technol.*, vol. 14, pp. 1153–1160, June 1996.
[9] H. Takesue, F. Yamamoto, K. Shimizu, and T. Horiguchi, "Stabilization of the pulsed lightwave circulating around an amplified fiber-optic ring incorporating a Lyot depolarizer," *IEEE Photon. Technol. Lett.*, vol. 10, pp. 1748–1750, Dec. 1998.
[10] H. Sabert and E. Brinkmeyer, "Passive birefringence compensation in a frequency comb generator based on a linear fiber optical delay line," *Electron. Lett.*, vol. 30, no. 10, pp. 812–814, 1994.
[11] H. Takesue, F. Yamamoto, and T. Horiguchi, "Stable lightwave synthesized frequency sweeper for the 1.5 μm band," in *Proc. Eur. Conf. Opt. Commun. ECOC'98*, paper WdA33.
[12] S. Yamashita and K. Hotate, "Single-polarization fiber laser composed of a normal single-mode erbium-doped fiber," in *Proc. Eur. Conf. Opt. Commun. ECOC'95*, paper We.P.34.
[13] Y. Takushima and K. Kikuchi, "Gain stabilization of all-optical gain-clamped amplifier by using Faraday rotator mirrors," *Electron. Lett.*, vol. 34, no. 5, pp. 458–459, 1998.
[14] Y. Takushima, S. Yamashita, K. Kikuchi, and K. Hotate, "Polarization-stable and single-frequency fiber lasers," *J. Lightwave Technol.*, vol. 16, pp. 661–669, Apr. 1998.
[15] K. Shimizu, T. Horiguchi, and Y. Koyamada, "Frequency translation of light waves by propagation around an optical ring circuit containing a frequency shifter: II. Theoretical analysis," *Appl. Opt.*, vol. 33, no. 15, pp. 3209–3219, 1994.
[16] H. Takesue, F. Yamamoto, K. Shimizu, and T. Horiguchi, "1 THz lightwave synthesized frequency sweeper with synchronously tuned bandpass filter," *Electron. Lett.*, vol. 34, no. 15, pp. 1507–1508, 1998.
[17] K. Shimizu, T. Horiguchi, and Y. Koyamada, "Continuous-wave frequency synthesis of a laser diode based on discrete-time negative frequency feedback: I. Experiment," *IEEE J. Quantum Electron.*, vol. 31, pp. 1038–1046, June 1995.

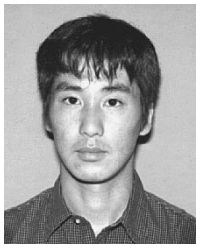

Hiroki Takesue was born in Wakayama, Japan on May 10, 1971. He received the B.E. and M.E. degrees in electrical engineering from Osaka University, Osaka, Japan, in 1994 and 1996, respectively.

In 1996, he joined NTT Access Network Service Systems Laboratories, Ibaraki, Japan. Since then, he has been engaged in research on lightwave frequency synthesis and WDM access networks.

Mr. Takesue is a member of the Institute of Electronics, Information and Communication Engineers (IEICE) of Japan.

Fumihiko Yamamoto was born in Yamaguchi, Japan, on January 25, 1966. He received the B.E. and M.E. degrees in mechanical engineering from Kyushu University, Fukuoka, Japan, in 1989 and 1991, respectively.

In 1991, he joined NTT Transmission Systems Laboratories, Ibaraki, Japan, where he has been engaged in research and development on in-service measurement technologies for optical access networks. He is now a Research Engineer of NTT Access Network Service Systems Laboratories, Ibaraki, Japan, where he works on WDM optical network design for metropolitan and local areas.

Mr. Yamamoto is a member of the Institute of Electronics, Information and Communication Engineers (IEICE) of Japan.

Tsuneo Horiguchi (M'87–SM'96) was born in Tokyo, Japan, on June 5, 1953. He received the B.E. and Dr.Eng. degrees from the University of Tokyo, Tokyo, Japan, in 1976 and 1988, respectively.

In 1976, he joined the NTT Ibaraki Electrical Communication Laboratories, where he worked on the measurement of the transmission characteristics of optical fiber cable. Since 1988, he has worked in the field of optical fiber distributed sensing. He is presently the Executive Manager of the Advanced Transmission Media Project, NTT Access Network Service Systems Laboratories, Ibaraki, Japan.

Dr. Horiguchi is a member of the Institute of Electronics, Information and Communication Engineers (IEICE) of Japan, the Optical Society of Japan, and the Optical Society of America (OSA).